

# Estimation of Fracture in Zirconia/AA2024 Alloy Particle-Reinforced Composites Subjected to Thermo-Mechanical Loading

<sup>1</sup>S. Sundara Rajan and A. Chennakesava Reddy<sup>2</sup>

<sup>1</sup>Scientist -G, Defence Research and Development Organisation, Hyderabad, India.

<sup>2</sup>Associate Professor, Department of Mechanical Engineering, Vasavi College of Engineering, Hyderabad, India  
dr\_acreddy@yahoo.com

**Abstract:** In the present work, the AA2024/ZrO<sub>2</sub> metal matrix composites were fabricated at 10% and 30% volume fractions of ZrO<sub>2</sub>. The composites were subjected to structural and thermal loads. The microstructure of AA2024 alloy/ZrO<sub>2</sub> reveals uniform distribution of ZrO<sub>2</sub> in the AA2024 alloy matrix. The transformation of ZrO<sub>2</sub> has not occurred from monoclinic to tetragonal due to thermal loading. Only interphase fracture has taken place in the composites.

**Keywords:** AA2024, zirconia, spherical nanoparticle, RVE model, finite element analysis, debonding.

## 1. INTRODUCTION

Many of the problems of special interest in the micromechanics domain are related to inclusions that are dispersed into an otherwise continuous phase. Of particular interest here are the cases of improving or optimizing stiffness and strength. Due to processing conditions and various surface treatments on the reinforced particles, an interfacial region is created between the particle and matrix in a particle reinforced composite material. In other words, a compliant bond almost always exists between the particle and the matrix. This region is of primary importance because it affects the quality of bonding and hence influences the structural performance of the overall composite material. The characterization of the interphase between the fiber and the matrix can be accomplished using either microscopic or micromechanics techniques, depending upon the dimensions as well as the type of composite system. Several microscopic techniques have been found to successfully characterize the interphase region. This includes destructive methods such as scanning electron microscope (SEM), scanning acoustic microscopy (SAM) [1]. It is known that many micromechanics models have been proposed to predict the effective mechanical properties of two-phase composites, such as the Mori–Tanaka model, differential method and generalized self-consistent method [2, 3]. The solution of one inclusion problem is the basis of these micromechanics models. However, the thickness of the thin interphase may become comparable to the size of the fillers for some cases, for example, where the fillers are nanoscale particles. Computational methods using finite element methods are the effective ways to study the micromechanical behavior of composite materials [4-20].

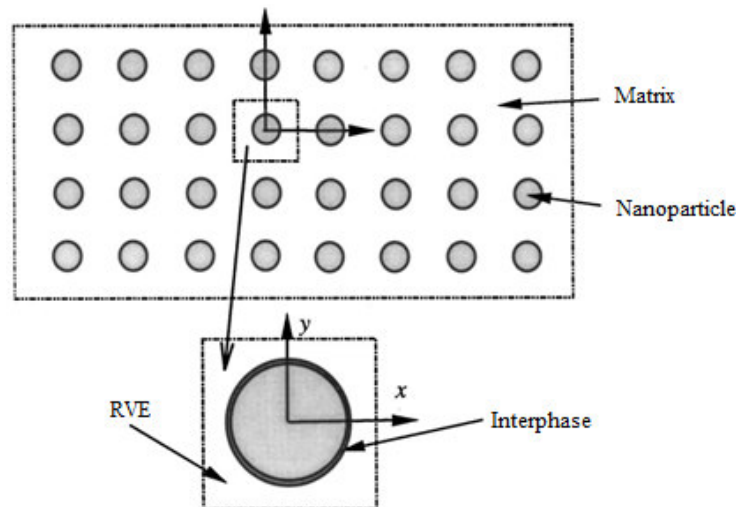


**Figure 1:** The interphase in a nanoparticle-reinforced composite.

Zirconia Powder (Zirconium Oxide, ZrO<sub>2</sub>) is synthesized from zircon sand (ZrO<sub>2</sub> · SiO<sub>2</sub>) using a solid-state reaction process. Zirconia has the common characteristics of ceramics that are not found in metallic or organic materials, including high

hardness (next to diamond), high mechanical strength, low coefficient of friction, high temperature stability, chemical resistance, erosion resistance, low electrical conductivity. Zirconium dioxide,  $ZrO_2$ , is used for optical coatings. Dense layers with exceptional hardness can be deposited by electron-beam evaporation or sputtering. Because of its hardness, it also finds common use as an abrasive material. In this paper, the effect of temperature on the fracture in AA2024 alloy/ $ZrO_2$  composites was investigated. The shape  $ZrO_2$  nanoparticle considered in this work is spherical. The periodic particle distribution was a square array as shown in figure 1. Both microscopic and micromechanics methods were employed in this paper.

## 2. MATERIALS METHODS

The matrix material was AA2024 alloy. The reinforcement material was  $ZrO_2$  nanoparticles of average size 100nm (figure 2). The mechanical properties of materials used in the present work are given in table 1.

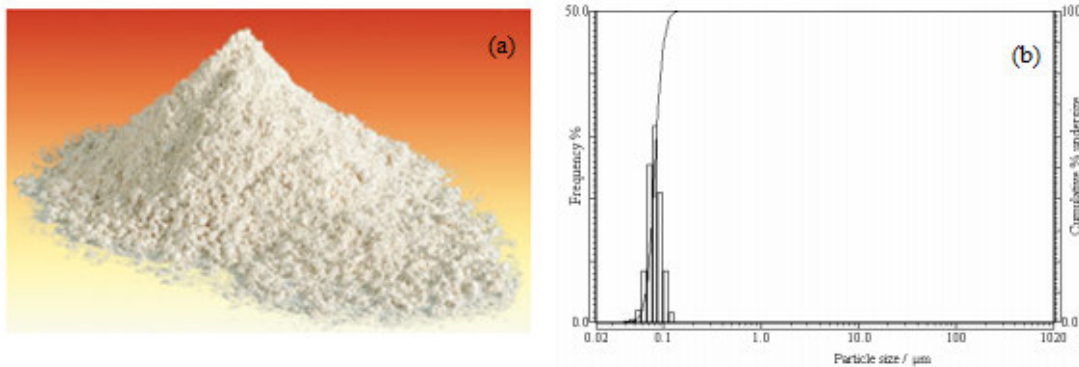


Figure 2: Zirconia nanopowder (a) and particle distribution (b).

Table 1: Mechanical properties of AA2024 matrix and  $ZrO_2$  nanoparticles

Property	AA2024	$ZrO_2$
Density, g/cc	2.71	5.5
Elastic modulus, GPa	72.49	250.0
Coefficient of thermal expansion, $10^{-6} 1/^\circ C$	20.8	7.5
Specific heat capacity, J/kg/ $^\circ C$	880	540
Thermal conductivity, W/m/ $^\circ C$	134	2.7
Poisson's ratio	0.33	0.32

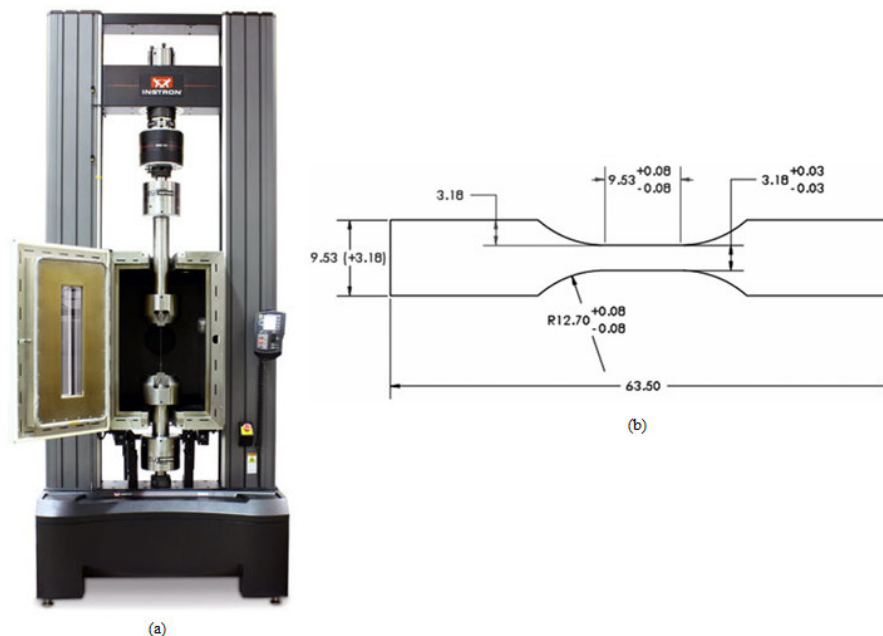


Figure 3: Tensile testing: UTM with temperature controlled chamber and (b) shape and dimensions of tensile specimen.

AA2024 alloy/  $ZrO_2$  composites were fabricated by the stir casting process and low pressure casting technique with argon gas at 3.0 bar. The composite samples were give solution treatment and cold rolled to the predefined size of tensile specimens. The heat-treated samples were machined to get flat-rectangular specimens (figure 3) for the tensile tests. The tensile specimens were placed in the grips of a Universal Test Machine (UTM) with temperature controlled chamber at a specified grip separation and pulled until failure. The test speed was 2 mm/min. A strain gauge was used to determine elongation. In the current work, a cubical representative volume element (RVE) was implemented to analyze the tensile behavior AA2024/  $ZrO_2$  nanoparticle composites at two (10% and 30%) volume fractions of  $ZrO_2$  and at different temperatures. The large strain PLANE183 element was used in the matrix in all the models. In order to model the adhesion between the matrix and the particle, a CONTACT 172 element was used.

### 3. RESULTS AND DISCUSSION

The optical micrograph as shown in figure 4 reveals random distribution of  $ZrO_2$  particles in AA2024 alloy matrix.

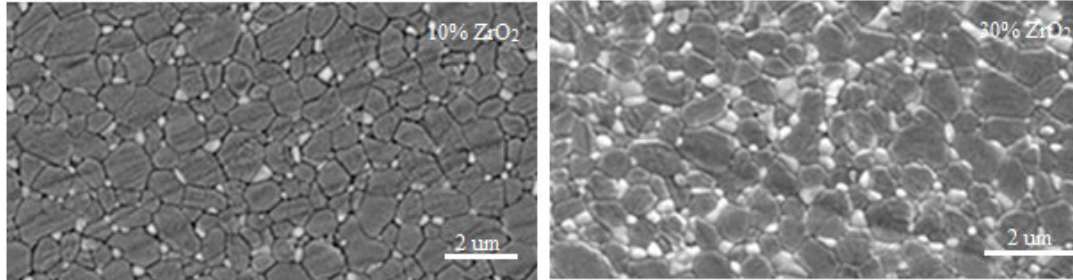


Figure 4: Microstructure showing distribution of  $ZrO_2$  nanoparticles in AA2024 alloy matrix.

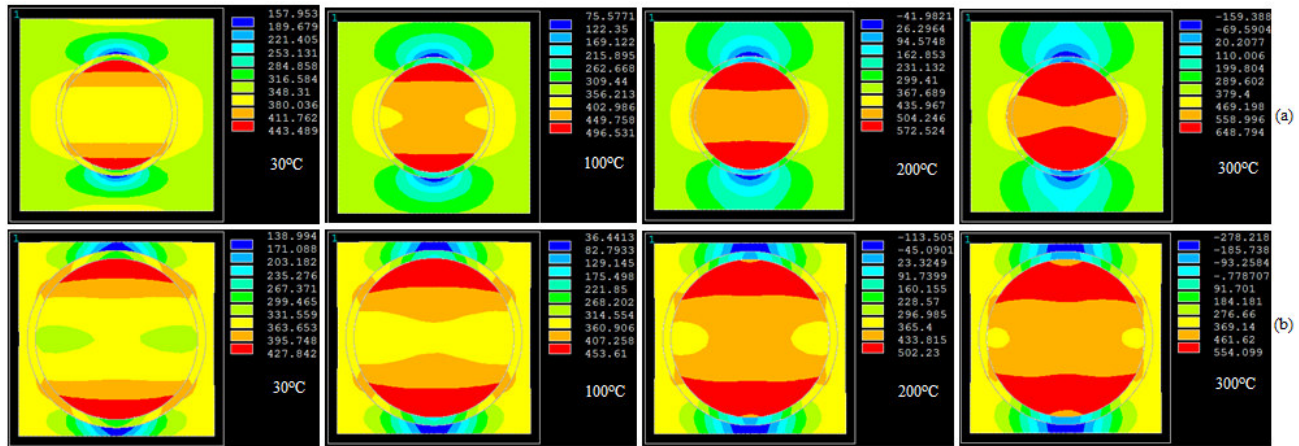


Figure 54: FEA results of tensile stress induced along load direction in the composites comprising of: (a) 10%  $ZrO_2$  and (b) 30%  $ZrO_2$ .

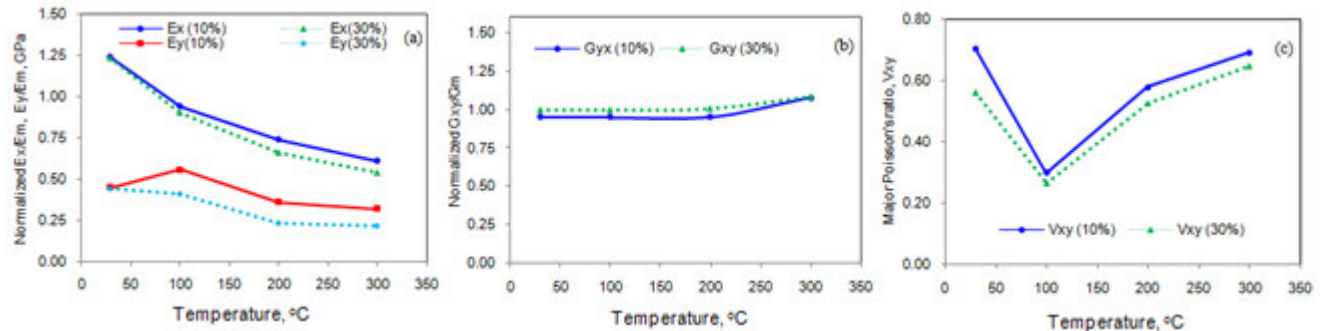


Figure 6: Effect of temperature on stiffness of AA2024/ $ZrO_2$  composites.

#### 3.1 Thermo-Mechanical Behavior

Figure 5 represents the tensile stresses induced in the AA2024/ $ZrO_2$  composites along the load direction. The tensile stress increases with increase of temperature and it decreases with increase of volume fraction of AA2024/ $ZrO_2$  in AA2024 alloy



matrix. This is due to softening of the composite with increase of temperature. The normalized elastic modulus is shown in figure 6a. The elastic modulus is normalized with the elastic modulus of AA2024 alloy. The stiffness of the composites decreases with increase of temperature. The stiffness of AA2024 alloy/10% ZrO<sub>2</sub> composites is higher than that of AA2024 alloy/30% ZrO<sub>2</sub> composites with respect to increase of temperature. The normalized stiffness along the normal direction is lower than that along the load direction. The normalized shear modulus increases with volume fraction of ZrO<sub>2</sub> (figure 6b). Initially, the major Poisson's ratio decrease from 30°C to 100°C and later on it increases with temperature from 100°C to 300°C (figure 6c).

### 3.2 Fracture Analysis

If the particle deforms in an elastic manner (according to Hooke's law) then,

$$\tau = \frac{n}{2} \sigma_p \tag{1}$$

where  $\sigma_p$  is the particle stress. If particle fracture occurs when the stress in the particle reaches its ultimate tensile strength,  $\sigma_{p,uts}$ , then setting the boundary condition at

$$\sigma_p = \sigma_{p, uts} \tag{2}$$

The relationship between the strength of the particle and the interfacial shear stress is such that if

$$\sigma_{p, uts} < \frac{2\tau}{n} \tag{3}$$

Then the particle will fracture. From the figure 7b, it is observed that the ZrO<sub>2</sub> nanoparticle was not fractured as the condition in Eq. (3) is not satisfied. For the interfacial debonding/yielding to occur, the interfacial shear stress reaches its shear strength:

$$\tau = \tau_{max} \tag{4}$$

For particle/matrix interfacial debonding can occur if the following condition is satisfied:

$$\tau_{max} < \frac{n\sigma_p}{2} \tag{5}$$

It is observed from figure 7a that the interfacial debonding occurs between ZrO<sub>2</sub> nanoparticle and AA2024 alloy matrix as the condition in Eq.(5) is satisfied. This is due to CTE mismatch between ZrO<sub>2</sub> nanoparticles and AA2024 alloy matrix.

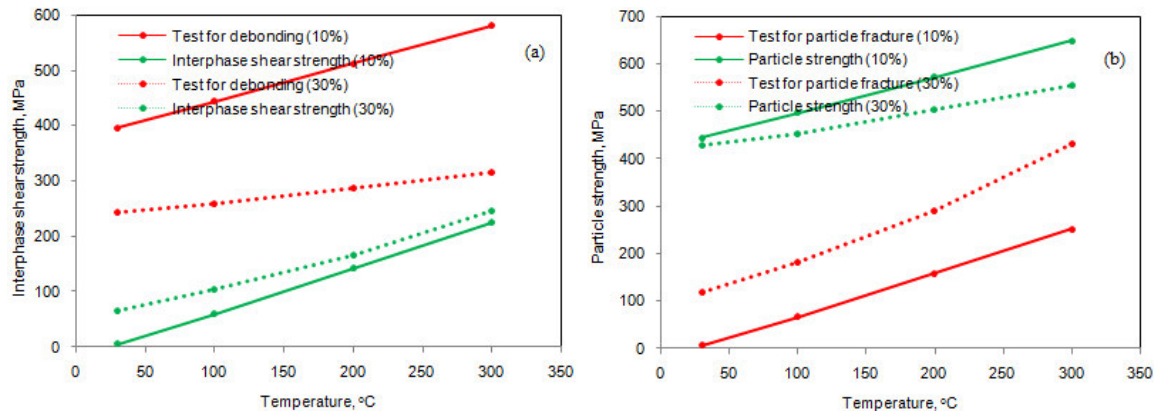


Figure 7: Criterion for interfacial debonding (a) and for particle fracture (b).

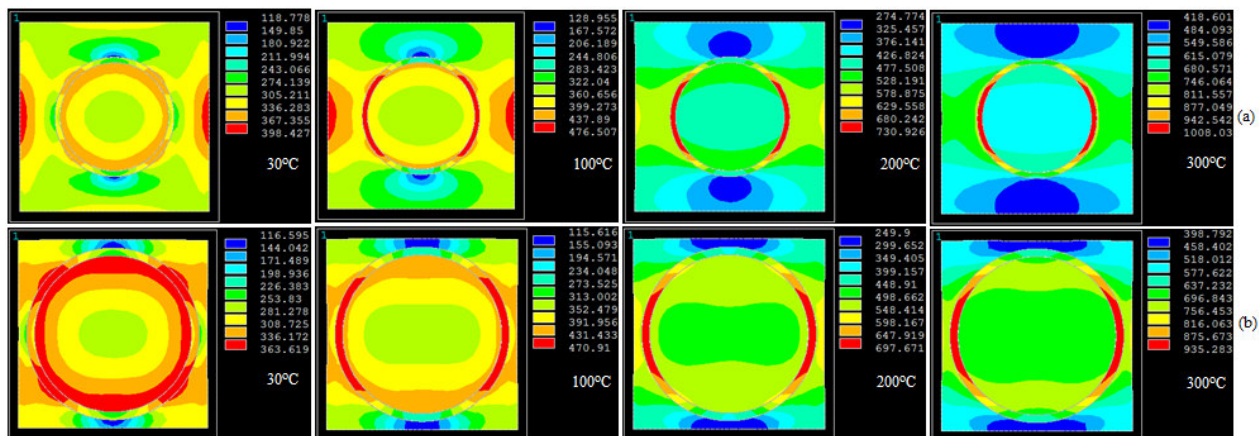


Figure 8: Images of von Mises stresses obtained from FEA: (a) AA2024/10% ZrO<sub>2</sub> and (b) AA2024/30% ZrO<sub>2</sub> composites.

The von Mises stress induced at the interface are higher than that induced in the nanoparticle (figure 8). Hence, the interfacial debonding was occurred between the particle and the matrix. The interfacial debonding increases with increase of temperature. Pure zirconium dioxide undergoes a phase transformation from monoclinic (stable at the room temperature) to tetragonal (at about 1173 °C) and then to cubic (at about 2370 °C), according to the scheme:

monoclinic (1173 °C)  $\leftrightarrow$  tetragonal (2370 °C)  $\leftrightarrow$  cubic (2690 °C)  $\leftrightarrow$  melt

As the test temperature is well below 1173°C, the transformation of ZrO<sub>2</sub> is not issue in the present work.

#### 4. CONCLUSION

The microstructure of AA2024 alloy/ ZrO<sub>2</sub> composites reveals the random distribution of ZrO<sub>2</sub> nanoparticles in the matrix. The shear stress is high at the interface resulting to interfacial debonding in AA2024/ ZrO<sub>2</sub> composites. The transformation of zirconia has not taken place from monoclinic to tetragonal due to thermal loading of composites.

#### REFERENCES

1. Y. Verma, et al., Acoustic microscopic investigation of the carbon fiber-polymer matrix interface in composites, Review of Progress in Quantitative Nondestructive Evaluation, 13, 1994, pp. 1493-1498.
2. R. M. Christensen, A critical evaluation for a class of micromechanics models, Journal of Mechanics and Physics of Solids 38, 1990, pp. 379-404.
3. R. W. Zimmerman, Elastic moduli of a solid containing spherical inclusions, Mechanics of Materials, 12, 1991, pp. 17-24.
4. J. D. Achenbach, H. Zhu, Effect of Interphases on Micro and Macromechanical Behavior of Hexagonal-Array Fiber Composites, ASME Journal of Applied Mechanics, 57, 1990, pp. 956-963.
5. A. Chennakesava Reddy, Effect of Particle Loading on Microelastic Behavior and interfacial Traction of Boron Carbide/AA4015 Alloy Metal Matrix Composites, 1st International Conference on Composite Materials and Characterization, Bangalore, March 1997, pp. 176-179.
6. A. Chennakesava Reddy, Reckoning of Micro-stresses and interfacial Traction in Titanium Boride/AA2024 Alloy Metal Matrix Composites, 1st International Conference on Composite Materials and Characterization, Bangalore, March 1997, pp. 195-197.
7. A. Chennakesava Reddy, Evaluation of Debonding and Dislocation Occurrences in Rhombus Silicon Nitride Particulate/AA4015 Alloy Metal Matrix Composites, 1st National Conference on Modern Materials and Manufacturing, Pune, India, 19-20 December 1997, pp. 278-282,.
8. A. Chennakesava Reddy, Interfacial Debonding Analysis in Terms of Interfacial Traction for Titanium Boride/AA3003 Alloy Metal Matrix Composites, 1st National Conference on Modern Materials and Manufacturing, Pune, 19-20 December, 1997.
9. A. Chennakesava Reddy, Assessment of Debonding and Particulate Fracture Occurrences in Circular Silicon Nitride Particulate/AA5050 Alloy Metal Matrix Composites, National Conference on Materials and Manufacturing Processes, Hyderabad, India, 27-28 February 1998, pp. 104-109.
10. A. Chennakesava Reddy, Local Stress Differential for Particulate Fracture in AA2024/Titanium Carbide Nanoparticulate Metal Matrix Composites, National Conference on Materials and Manufacturing Processes, Hyderabad, India, 27-28 February 1998, pp. 127-131.
11. A. Chennakesava Reddy, Micromechanical Modelling of Interfacial Debonding in AA1100/Graphite Nanoparticulate Reinforced Metal Matrix Composites, 2nd International Conference on Composite Materials and Characterization, Nagpur, India, 9-10 April 1999, pp. 249-253.
12. A. Chennakesava Reddy, Cohesive Zone Finite Element Analysis to Envisage Interface Debonding in AA7020/Titanium Oxide Nanoparticulate Metal Matrix Composites, 2nd International Conference on Composite Materials and Characterization, Nagpur, India, 9-10 April 1999, pp. 204-209.
13. B. Kotiveera Chari, A. Chennakesava Reddy, Debonding Microprocess and interfacial strength in ZrC Nanoparticle-Filled AA1100 Alloy Matrix Composites using RVE approach, 2nd National Conference on Materials and Manufacturing Processes, Hyderabad, India, 10-11 March 2000, pp. 104-109.
14. A. Chennakesava Reddy, Micromechanical and fracture behaviors of Ellipsoidal Graphite Reinforced AA2024 Alloy Matrix Composites, 2nd National Conference on Materials and Manufacturing Processes, Hyderabad, India, 10-11 March 2000, pp. 96-103.
15. S. Sundara Rajan, A. Chennakesava Reddy, Micromechanical Modeling of Interfacial Debonding in Silicon Dioxide/AA3003 Alloy Particle-Reinforced Metal Matrix Composites, 2nd National Conference on Materials and Manufacturing Processes, Hyderabad, India, 10-11 March 2000, pp. 110-115.

16. S. Sundara Rajan, A. Chennakesava Reddy, Role of Volume Fraction of Reinforcement on Interfacial Debonding and Matrix Fracture in Titanium Carbide/AA4015 Alloy Particle-Reinforced Metal Matrix Composites, 2nd National Conference on Materials and Manufacturing Processes, Hyderabad, India, 10-11 March 2000, 116-120.
17. A. Chennakesava Reddy, Constitutive Behavior of AA5050/MgO Metal Matrix Composites with Interface Debonding: the Finite Element Method for Uniaxial Tension, 2nd National Conference on Materials and Manufacturing Processes, Hyderabad, India, 10-11 March 2000, pp. 121-127.
18. B. Kotiveera Chari, A. Chennakesava Reddy, Interfacial Debonding of Boron Nitride Nanoparticle Reinforced 6061 Aluminum Alloy Matrix Composites, 2nd National Conference on Materials and Manufacturing Processes, Hyderabad, India, 10-11 March 2000, pp. 128-133.
19. P. M. Jebaraj, A. Chennakesava Reddy, Simulation and Microstructural Characterization of Zirconia/AA7020 Alloy Particle-Reinforced Metal Matrix Composites, 2nd National Conference on Materials and Manufacturing Processes, Hyderabad, India, 10-11 March 2000, pp. 134-140.
20. P. M. Jebaraj, A. Chennakesava Reddy, Continuum Micromechanical modeling for Interfacial Debonding of TiN/AA8090 Alloy Particulate Composites, 2nd National Conference on Materials and Manufacturing Processes, Hyderabad, India, 10-11 March 2000, pp. 141-145.